

Phase diagram at $T=0$ of the one-dimensional chiral planar model in a twofold-anisotropy field

M. Hébert, A. Caillé, and A. Bel Moufid

Centre de Recherche en Physique du Solide et Département de Physique, Université de Sherbrooke, Sherbrooke, Québec, Canada J1K 2R1

(Received 13 January 1993; revised manuscript received 25 March 1993)

The ground-state phase diagram for the one-dimensional chiral planar model in a twofold-anisotropy field is obtained. An intrinsic reflection-symmetry property about the natural angle of cantedness $\Delta = \pi/2$ is demonstrated and serves to relate commensurate phases having different orders of commensurability. This last property is used to establish a comparison with earlier results obtained by A. Banerjee and P. L. Taylor [Phys. Rev. B **30**, 6689 (1984)]. The phase boundaries at low amplitude of the twofold-anisotropy field are determined analytically with a criterion of zero creation energy of isolated solitons. At finite value of the amplitude of the anisotropy field, the phase diagram is obtained with an effective potential.

I. INTRODUCTION

The ground-state phase diagram of the one-dimensional chiral planar model in a twofold-anisotropy field has been studied previously by Banerjee and Taylor.¹ In their treatment, they restricted the angle Δ measuring the natural cantedness of the system to the first quarter of the full circle and imposed an additional indistinguishability between polar angles differing by π , having in mind an application to polytetrafluoroethylene crystalline polymers.² These limitations are too restrictive for the planar vector model and leave out half of the phase diagram with phases having a specific order of commensurability. As is shown later, an interesting mirror symmetry about $\Delta = \pi/2$ exists, relating phases of different orders of commensurability. In addition to the above, it is worth mentioning that a planar model, in a twofold-anisotropy field, which does not differentiate between θ and $\theta + \pi$ in its nearest-neighbor potential energy would be turned³ into a vector model in a magnetic field. Under these conditions we know the phase diagram to be very different,⁴ making extensive use of the nonconvex part of the interparticle potential energy. In the present study, we have in mind applications^{3,5} to the one-dimensional discotic liquid-crystal phases having at their lattice sites physical quantities possessing intrinsic threefold rotational symmetry embedded either in a sixfold or threefold local anisotropy field. These applications call for an extensive study of the phase diagram of the chiral planar model in a twofold-anisotropy field, the case of a onefold-anisotropy field having received an extensive treatment⁴ in the past.

The rest of this paper is organized as follows. The model potential energy is presented in Sec. II with a study of its symmetry properties. It is followed in Sec. III by the determination of the boundaries at small amplitude of the anisotropy field and of the principal commensurate phases, with a criterion of zero creation energy of a single soliton in an otherwise commensurate phase. In Sec. IV, the complete phase diagram at a

higher value of the anisotropy field is obtained using the method of effective potential of Griffiths and Chou.⁶ Finally, a discussion of the results and conclusions are presented in Sec. V.

II. THE MODEL AND ITS SYMMETRY PROPERTIES

The potential energy of the chiral planar model is written as follows:

$$E(\theta_n) = \sum_n \left[-\cos(\theta_n - \theta_{n-1} - \Delta) - \frac{H}{2} \cos(2\theta_n) \right], \quad (1)$$

where θ_n is the angle between the vector at site n and a preferred fixed direction in the plane of the vectors. H is the amplitude of the twofold-anisotropy field relative to a unit amplitude for the nearest-neighbor intersite chiral interaction. Δ is a measure of the natural angle between nearest neighbors. This potential energy has a few symmetry properties which are used to limit the parameter space for a thorough study of the phase diagram. It is easily shown that

$$E[\Delta, H, (\theta_n)] = E[\Delta + 2\pi, H, (\theta_n)], \quad (2a)$$

$$= E[-\Delta, H, (-\theta_n)], \quad (2b)$$

$$= E[\Delta, -H, (\theta_n + \pi/2)], \quad (2c)$$

$$= E[\pi - \Delta, H, (n\pi - \theta_n)]. \quad (2d)$$

Equation (2d) expresses an additional nontrivial symmetry of $E(\theta_n)$ which relates commensurate phases linked by a mirror reflection about $\Delta = \pi/2$. In order to specify the commensurate phases related by (2d), we use the notation introduced by Yokoi, Tang, and Chou.⁴ The average nearest-neighbor intermolecular angular displacement is written as follows:

$$\langle \theta_{n+1} - \theta_n \rangle = q = 2\pi\bar{q}. \quad (3)$$

For certain ranges of the parameter Δ at a given H , com-

commensurate phases are obtained having $P2\pi$ rotations for the Q successive vectors of an entire period. The rational number

$$\bar{q} = P/Q \quad (4)$$

is used to specify the order of the commensurate phase. The above reflection symmetry property about $\Delta = \pi/2$ imposes the condition that the commensurate phase P/Q for $\Delta > \pi/2$ occupies a domain of the parameter space which is the mirror image about $\Delta = \pi/2$ of the commensurate phase P'/Q' for $\Delta < \pi/2$; the orders of commensurability being related by

$$\frac{P}{Q} = \left[\frac{Q' - 2P'}{2Q'} \right]_r \quad (5)$$

(r), is used to specify the rational number in its reduced form. Contrary to the onefold-anisotropy field,⁴ only phases with the reduced form of P/Q were observed in the twofold-anisotropy field. As a result of the symmetry properties [Eqs. (2) and (5)], it is sufficient to consider the phase diagram for $H > 0$ and $\pi/2 < \Delta < \pi$.

In the absence of an anisotropy field, a perfect helical ordering of a definite chirality is obtained with $\langle \theta_{n+1} - \theta_n \rangle = \Delta$, where an infinite succession of commensurate and incommensurate phases occurs with increasing Δ . Contrary to a model with discrete spins, like the ANNNI model,⁷ the twist q of the helix varies continuously, like in a floating phase⁷ not pinned to the lattice at $H = 0$, and the incommensurate phases occupy the full domain of the Δ parameter space leaving a space of zero measure for the commensurate phases.

The presence of a finite amplitude H for the anisotropy field introduces domains of finite width in the Δ parameter space for the commensurate phases, turning the phase diagram into a harmless, complete or incomplete, Devil's staircase. These behaviors will be studied both analytically at small H and numerically for all values of H in Secs. III and IV, respectively. At this point, let us illustrate the behavior in the limit of an infinite amplitude H of the anisotropy field. In this limit the vector angles are limited to $\theta_n = 0$ and $\theta_n = \pi$. The ground-state energies of the ferromagnetic phase 0/1 and the antiferromagnetic phase 1/2 are equal at $\Delta = \pi/2$, the ferromagnetic and antiferromagnetic phases being ground states, respectively, for $\Delta < \pi/2$ and $\Delta > \pi/2$. At $\Delta = \pi/2$, phase generated from the ferromagnetic phase by reversing one or many vectors have the same energy as the ferromagnetic or antiferromagnetic phases. The character of the phase at the limiting point $\Delta = \pi/2$ and $H \rightarrow \infty$ is of interest. Starting from the ferromagnetic phase 0/1 and reversing vectors, any commensurate phase P/Q with a higher order of commensurability may be formed without any cost in energy. Random phases with their periods approaching infinity may also be generated. In this Ising limit, the absence of a continuous character for the site variables prevents the appearance of incommensurate phases. We thus conclude that the limiting point $H \rightarrow \infty$ and $\Delta = \pi/2$ is a multiphase point of the kind predicted in the ANNNI model.⁷

III. SOLITON INSTABILITY STUDY FOR SMALL H

We now study the limit of stability of certain commensurate phases at weak but finite values of the amplitude H of the anisotropy field. We will assume that the limit of stability is signaled by the vanishing of the creation energy of a single soliton in an otherwise commensurate phase. Starting with the uniform ferromagnetic phase 0/1, and measuring the energy with respect to this phase, the total-energy difference becomes

$$\Delta E(\theta_n) = \sum_n [1 - \cos(\theta_{n+1} - \theta_n - \Delta)] + H \sum_n \sin^2 \theta_n \quad (6)$$

For $H \ll 1$ and Δ near zero, treating the angular variable $\theta(n)$ as a slowly varying continuous function of n , ΔE becomes

$$\Delta E(\theta_n) \simeq -\Delta[\theta(\infty) - \theta(-\infty)] + \int_{-\infty}^{+\infty} dn \left[\frac{1}{2} \left[\frac{d\theta}{dn} \right]^2 + H \sin^2[\theta(n)] \right] \quad (7)$$

Solving the differential equation obtained from the extremal condition of the energy functional (7), with the boundary conditions at infinity $\theta(\pm\infty) = 0$ or π , the following soliton (+) and antisoliton (-) are obtained.

$$\theta(n) = 2 \tan^{-1} \{ \exp[\pm(2H)^{1/2} n] \} \quad (8)$$

The creation energy of the soliton and antisoliton are, respectively,

$$\Delta E = \frac{4}{\sqrt{2}} H^{1/2} \mp \pi \Delta \quad (9)$$

For $|\Delta| \geq \Delta_c [\Delta_c = (4/\pi\sqrt{2})H^{1/2}]$, the ferromagnetic phase 0/1 is unstable for the creation of solitons ($\Delta > 0$) or antisolitons ($\Delta < 0$). It may be easily shown that in the antiferromagnetic phase 1/2, the lines of instability for Δ near $\pm\pi$ are given by

$$\Delta = \pm\pi \mp \frac{4}{\sqrt{2}} H^{1/2} \quad (10)$$

We now study the stability of the 1/4 phase near $\Delta = \pi/2$. In the 1/4 phase, the angular variable θ_n is written as follows:

$$\theta_n = \frac{\pi}{2} n + \phi + \xi_n \quad (11)$$

For $H = 0$, the global phase angle ϕ is undetermined and the modulation $\xi_n = 0$. For $H \neq 0$, ϕ is fixed and a finite value of the modulation ξ_n develops. Modulations with wave numbers π and $\pi/2$, both being compatible with $q = \pi/2$, ξ_n is written as follows:

$$\xi_n = (-1)^n x + y \cos \left[n \frac{\pi}{2} \right] + z \sin \left[n \frac{\pi}{2} \right] \quad (12)$$

To the lowest order in x, y, z , and H , the energy per site is minimal for

$$x \simeq -\frac{H \sin(2\phi)}{2 \sin(\Delta)} + O(H^3), \quad (13)$$

$$y \simeq O(H^3),$$

and

$$z \simeq O(H^3).$$

Substituting (13) in the energy per site ε , we obtain

$$\varepsilon \simeq 1 - \sin(\Delta) + H - \frac{1}{2} \frac{H^2 \sin^2(2\phi)}{\sin(\Delta)} + O(H^3). \quad (14)$$

The last term in H^2 favors $\phi = \pi/4$, an infinitesimal H , fixing the vectors in the middle of each quadrant in the distorted phase of period 4. To order H^2 , the angular variables in the distorted phase of period 4 are given by

$$\theta_n \simeq \frac{\pi}{2}n + \frac{\pi}{4} - \frac{H}{2}(-1)^n + O(H^3). \quad (15)$$

This distorted period 4 may be looked upon as a double fan phase, with pairs of successive vectors being drawn together alternatively towards $\theta=0$ and $\theta=\pi$. We study the stability of the distorted period 4 phase using a method similar to the one presented for the uniform phase $0/1$. The soliton and antisoliton, appearing as a slow variation of the phase angle ϕ , are, respectively,

$$\phi(n) = \frac{\pi}{4} + 2 \tan^{-1} \left\{ \exp[\pm(2H)^{1/2}n] \right\}. \quad (16)$$

The soliton and antisoliton have, respectively, zero creation energy for

$$H = 2\pi^2 \left[\pm \frac{\Delta}{2\pi} \mp \frac{1}{4} \right]. \quad (17)$$

According to Bak,⁸ the commensurate phase P/Q should become unstable with respect to the creation of isolated solitons for

$$\frac{\Delta}{2\pi} - \frac{P}{Q} \simeq H^{Q/2}. \quad (18)$$

At first, the above result (17) seems not to agree with Bak's result. This is only apparent; the two may be reconciled when one observes that to lowest order, it is the $Q=2$ modulation ($x \neq 0$) which is nonzero in our case.

We have also conducted a similar calculation for the phase of period 3 near $\Delta = 2\pi/3$. To lowest order in H , the distorted phase of period 3 is given by

$$\theta_n = \frac{2\pi}{3}n + \phi + \frac{H}{3} \sin \left[\frac{2\pi}{3}n - 2\phi \right]. \quad (19)$$

The phase angle ϕ is shown to be fixed at $\phi=0$ or $\phi=\pi/3$, these two states being fully equivalent with a single vector pointing either up or down in a given period. The distorted phase of period 3 becomes unstable with respect to the creation of solitons or antisolitons (in ϕ_n) at

$$\Delta = \frac{2\pi}{3} \left[1 - \frac{\sqrt{3}H^2}{12\pi} \mp \frac{H^{3/2}}{\pi^2} \right]. \quad (20)$$

The lines of instability (10), (17), and (20) are plotted on Fig. 1 where the full diagram obtained by the numerical method used in Sec. IV is presented.

IV. PHASE DIAGRAM USING THE EFFECTIVE POTENTIAL METHOD

A very useful method to obtain the general features of the ground-state phase diagram of a one-dimensional system with competing interactions is the algorithm of Griffiths and Chou.⁶ In principle, the ground-state phase diagram of the potential energy (1) could be obtained through a search for the extremal conditions,

$$\frac{\partial E(\theta_n)}{\partial \theta_n} = 0. \quad (21)$$

However, this procedure could be very misleading since it points not only to minimal energy states but to all extremal energy states. Additional complications of nonuniqueness arise when the interparticle potential is nonconvex.⁹ In comparison to this, the use of the effective potential method focuses directly on the ground state. Extensively used and well described in the literature,^{4,6,10-12} this technique finds its justification as the zero-temperature limit of the transfer operator,

$$\hat{T}(u', u) = \exp \left\{ -\frac{\beta}{2} [V(u) + V(u')] - \beta W(u' - u) \right\}, \quad (22)$$

where u and $u' \in [0, 1]$ and β is the inverse temperature. $V(u')$ and $W(u' - u)$ are, respectively, the intersite and nearest-neighbor intersite potentials. The corresponding eigenvalue problem can be expressed as follows:

$$\int du \hat{T}(u', u) e^{-\beta R(u)} = e^{-\beta \lambda} e^{-\beta R(u')}, \quad (23)$$

where $e^{-\beta R(u)}$ and $e^{-\beta \lambda}$ are, respectively, the left eigenfunction and eigenvalue. In the $T \rightarrow 0$ limit, the integral is dominated by the maximum of the integrand, giving

$$\lambda + R(u') = V(u') + \min_u [W(u', u) + R(u)] = KR(u'). \quad (24)$$

A similar equation holds for the right eigenfunction. In this context $R(u)$, which possesses the same period as $V(u)$, is called the "effective potential" and λ is the ground-state energy per site. It has been shown⁶ that (24) admits a unique solution for $R(u)$ and λ , with λ real and positive. The power of the algorithm, which is not yet fully understood, lies in its easy numerical implementation. The process of finding $R(u)$ is iterative, and the scheme, suggested by (24), that gives the best convergence⁴ is

$$R^{(j+1)}(u) = \frac{1}{2} [KR^{(j)}(u) + R^{(j)}(u)] - \lambda^{(j)}. \quad (25)$$

$R^{(j)}(u)$ is the effective potential, discretized in v equidistant points ($v \simeq 10^3$), at the j th iteration, and $\lambda^{(j)}$ is chosen so that

$$\min_u [KR^{(j+1)}(u)] = 0. \quad (26)$$

This technique converges quickly, with weak dependence on the initial conditions [for example $R^{(0)}(u) = V(u)$]. The recursion is stopped when the following self-

consistency is reached;

$$\max_u (|R^{(j+1)}(u) - R^{(j)}(u)|) < \epsilon, \quad (27)$$

with ϵ arbitrarily small (we used $\epsilon \approx 10^{-6} - 10^{-8}$). The effective potential calculated using (24) defines a mapping,

$$u = M(u'), \quad (28)$$

representing the ground-state configuration. It is constructed in such a way that for each u' one assigns the point u for which the right-hand side of (24) is minimal. After a transient state, the mapping tends to an attractor. The physical particle arrangement is then given by

$$u_{n-1} = M(u_n). \quad (29)$$

The H - Δ phase diagram of (6) is obtained as follows. At each point $(H, \Delta/2\pi)$, one generates the effective potential (with proper discretization and within given precision), calculates the mapping (28), and the ground-state configuration. To identify the order of commensurability

of the phase associated to that point, the winding number ω defined¹³ by

$$\omega = \frac{1}{m} \sum_{n=1}^m \Theta(u_{n-1} - u_n), \quad (30)$$

is calculated, where Θ is the Heaviside step function.

Figure 1 shows the full phase diagram obtained by this method for $\pi/2 < \Delta < \pi$. It is made of tongues starting at commensurate values of the twist of the helix on the $H=0$ axis and extending to $H \rightarrow \infty$ to merge into the multiphase point described above. It is to be noticed that for $H > 3$, most of the phase diagram is occupied by three phases 1/4, 1/3, and 1/2. However, it is conjectured (the numerical method is not able to obtain higher-order commensurate or incommensurate phases) that all commensurate phases exist for the entire domain of H , giving rise to a complete Devil's staircase. We have also verified that all phases are convex, in agreement with previous conjectures.⁶

V. DISCUSSIONS AND CONCLUSIONS

At this point, it is important to compare these results with those obtained by Banerjea and Taylor.¹ As indicated above, a set of tongues obtained from the mirror image of Fig. 1 about $\Delta = \pi/2$ will compose the phase diagram for $0 < \Delta < \pi/2$. The order of commensurability of the obtained phases are given by Eq. (5). The phase boundaries are in excellent quantitative agreement with those obtained numerically by Banerjea and Taylor.¹ However, the order of commensurability has to be revised, giving successively 1/10, 1/8, 1/6, 1/5, and phase 1/4 occupying the center of the phase diagram around $\pi/2$.

In Fig. 1, we have also plotted the phase boundaries obtained from the criterion of instability of the spontaneous creation of isolated solitons. At low H ($H < 0.5$), the agreement is excellent with the numerical results and serves to help one understand the origin of the bulging of tongues delimiting the area occupied by a phase of a given order of commensurability at low H . The discussion of phase 1/4 will illustrate this very well. As shown above, the application of an infinitesimal amplitude H of the anisotropy field fixes the phase angle ϕ of the period 4 phase at $\pi/4$, destroying the rotational invariance in the plane of the vectors. Further increasing H turns the pinned period 4 phase into a distorted double structure fan phase, allowing the existence of a commensurate phase of order 4 away from the natural twist of $\Delta = \pi/2$. Equivalent phase angle pinning is seen for phase 1/3 and the effect is maximum for the antiferromagnetic phase 1/2, where the pinning at $\phi = 0$ or π allows the phase to occupy most of the phase diagram at larger values of H .

At this point, it is interesting to compare the results for a twofold-anisotropy field with that of a onefold-anisotropy field of Yokoi, Tang, and Chou.⁴ As seen by these authors (Fig. 4 of Ref. 4), the application of the onefold-anisotropy field breaks the symmetry about $\Delta = \pi/2$, forcing the occupation of the nonconvex part of the interparticle potential at higher values of the anisotropy field and finally imposing a locking effect which leaves only two phases at $H \geq 2$ with a second-order

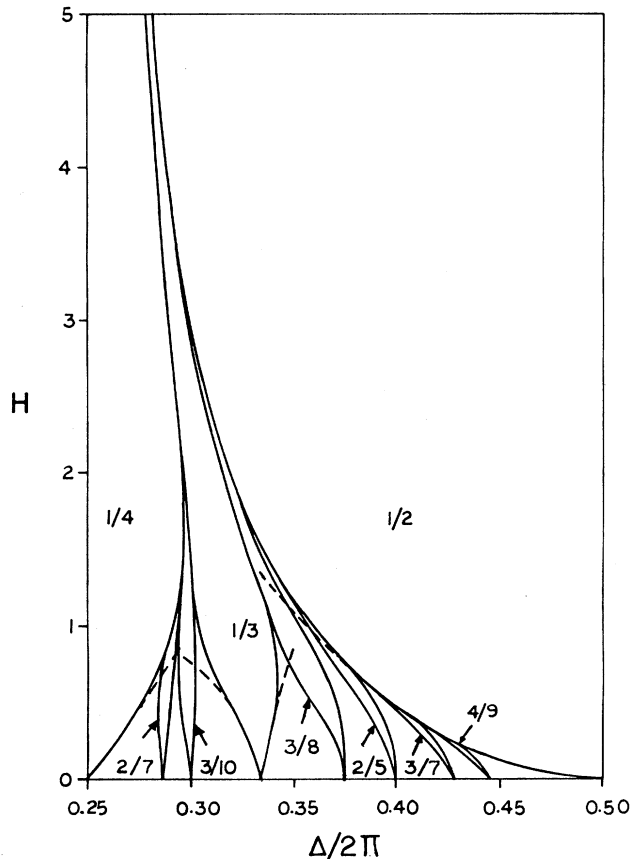


FIG. 1. The H - Δ ground-state phase diagram for $\pi/4 < \Delta < \pi/2$. The phase boundaries obtained analytically from Eqs. (10), (17), and (20) are shown by dashed lines. The different phases are characterized by their commensurability order P/Q , the arrows pointing at the tongue of a particular phase. The full curves were obtained numerically by the effective potential method.

phase transition between the two with increasing Δ . In addition to this, there is an overall tendency for the tongues describing the commensurate phase to incline to the right in parameter space. Compared to this, the phase diagram of the twofold-anisotropy field retains its symmetry with respect to $\Delta = \pi/2$, with all tongues for the commensurate phases inclined to converge towards this value of Δ in the phase diagram. This result will be used in a further paper³ to understand the behavior of

one-dimensional strands of discotic liquid crystals in different types of local environments.

ACKNOWLEDGMENTS

We thank M. L. Plumer for useful discussions on this problem. This work was supported by the Natural Sciences and Engineering Research Council (NSERC) of Canada and the Fonds pour la Formation des Chercheurs et d'Aide à la Recherche (FCAR) du Québec.

¹A. Banerjea and P. L. Taylor, *Phys. Rev. B* **30**, 6689 (1984).

²J. J. Weeks, I. C. Sanchez, R. K. Eby, and C. I. Poser, *Polymer* **21**, 325 (1980), and references therein.

³A. Caillé and M. Hébert (unpublished).

⁴C. S. O. Yokoi, L. H. Tang, and W. Chou, *Phys. Rev. B* **37**, 2173 (1988).

⁵E. Fontes, P. A. Heiney, and W. H. de Jeu, *Phys. Rev. Lett.* **61**, 1202 (1988).

⁶R. B. Griffiths and W. Chou, *Phys. Rev. Lett.* **56**, 1229 (1986); *Phys. Rev. B* **34**, 6219 (1986).

⁷J. Yeomans, *Solid State Phys.* **41**, 151 (1988).

⁸P. Bak, *Rep. Prog. Phys.* **45**, 587 (1982).

⁹S. Aubry, *Physica D* **7**, 240 (1983); S. Aubry and P. Y. LeDea-ron, *ibid.* **8**, 381 (1983).

¹⁰K. Sasaki and L. M. Floria, *J. Phys. Condens. Matter* **1**, 2179 (1989).

¹¹K. Hood, *J. Comput. Phys.* **89**, 187 (1990).

¹²L. M. Floria and R. B. Griffiths, *Numer. Math.* **55**, 565 (1989).

¹³M. Marchand, K. Hood, and A. Caillé, *Phys. Rev. Lett.* **58**, 1660 (1987).